Published in final edited form as:
Dev Dyn. 2010 March ; 239(3): 844–854. doi:10.1002/dvdy.22216.

Fibromodulin Regulates Collagen Fibrillogenesis During Peripheral Corneal Development

Shoujun Chen[a], **Ake Oldberg**[b], **Shukti Chakravarti**[c], and **David E. Birk**[a,*]

[a]Department of Pathology & Cell Biology, University of South Florida, College of Medicine, Tampa, FL

[b]Experimental Medical Sciences, University of Lund, Lund Sweden

[c]Department of Medicine, Johns Hopkins University School of Medicine, Baltimore, MD

Abstract

Fibromodulin regulates collagen fibrillogenesis, but its existence/role(s) in the cornea is controversial. We hypothesize that fibromodulin regulates fibrillogenesis during postnatal development of the anterior eye. Fibromodulin is weakly expressed in the limbus at post-natal day (P) 4; increases and extends into the central cornea at P14; becomes restricted to the limbus at P30 and decreases at P60. This differential spatial and temporal expression of fibromodulin is coordinated with emmetropization; the developmental increase in axial length and globe size. Genetic analysis demonstrated that fibromodulin regulates fibrillogenesis in a region specific manner. At the limbus, fibromodulin is dominant in regulating fibril growth during postnatal development. In the posterior peripheral cornea, cooperative interactions of fibromodulin and lumican regulate fibrillogenesis. These data indicate that fibromodulin plays important roles in the regulation of region-specific fibrillogenesis required for the integration of the corneal and scleral matrices and sulcus development required for establishment of the visual axis.

Keywords

Cornea; limbus; eye development; collagen fibril assembly; proteoglycans; Fibromodulin

Introduction

The cornea and sclera form the outer most portion of the eye and in both, type I collagen fibrils are the primary structural element. However, there are distinct differences in fibril structure, organization, and function in these two adjacent tissues. Fibrils in the corneal stroma have homogeneous, small diameters, regular packing into layers with an orthogonal organization. This precise organization is required for mechanical strength and corneal transparency. In contrast, fibrils in sclera are much larger in diameter, have a heterogeneous distribution of diameters, are organized into fibers that are interwoven (Rada et al., 2006). As a result, the sclera is opaque, but can bear more mechanical stress than the cornea. At the limbus the integration of these structurally and functionally different tissues gives two different curvatures, forming the scleral sulcus where the cornea joins the sclera. Disruption of collagen fibrillogenesis in this region is associated with abnormal curvatures, leading to refractive errors (Derdoy, 1968).

*Address correspondence to: David E. Birk, Ph.D., Department of Pathology & Cell Biology, University of South Florida, College of Medicine, 12901 Bruce B. Downs Blvd., MDC11, Tampa, FL 33612-4799, Tel# 813 974-8598, Fax# 813 974-5536, dbirk@health.usf.edu.

Small leucine-rich proteoglycans (SLRPs) are a group of extracellular matrix molecules with common structural and functional properties (Schaefer and Iozzo, 2008). In the human, several SLRP-linked genetic diseases have been reported recently. Loss of function mutations in SLRPs encoding genes such as lumican, fibromodulin, PRELP and opticin have been linked with high myopia (Wang et al., 2006; Majava et al., 2007). A frameshift mutation of decorin causing a C-terminal 33 amino acid deletion has been found in congenital stromal dystrophy of the cornea (Bredrup et al., 2005; Rodahl et al., 2006). Missense and frameshift mutations in keratocan, leading to a single amino acid substitution or a C-terminal truncation, caused cornea plana (CNA2) (Pellegata et al., 2000). Mouse models have demonstrated that SLRP deficient tissues have a disruption of fibril structure, organization and tissue structure resulting in a variety of phenotypes including: skin laxity (Danielson et al., 1997), corneal opacity (Chakravarti et al., 1998), weak tendons (Svensson et al., 1999) and altered mineralization (Goldberg et al., 2006). Increasing evidence indicates that differential expression and cooperation of different SLRPs are involved in assembly of tissue-specific structure and function (Chakravarti et al., 2006; Zhang et al., 2009).

A recent study demonstrated a severe fibril and stromal phenotype in compound decorin and biglycan deficient mice (Zhang et al., 2009). The single null mice had relatively normal corneal stromas. Fibrillogenesis assays revealed that decorin has a primary role in regulating fibril assembly, while biglycan can compensate for the loss of decorin in early development. Interaction of lumican driving keratocan expression in the cornea has also been reported (Carlson et al., 2005). Fibromodulin and lumican show 47% identity in primary sequence and bind the same site on type I collagen (Svensson et al., 2000; Kalamajski and Oldberg, 2009). Both fibromodulin (Matheson et al., 2005; Goldberg et al., 2006) and lumican (Chakravarti et al., 2006) are involved in regulation of fibrillogenesis in a tissue-specific manner. In addition, it was demonstrated in tendon, that lumican was increased in the absence of fibromodulin (Svensson et al., 1999; Chakravarti et al., 2003), suggesting they function as a closely coordinated pair as is the case for decorin and biglycan.

The cornea and sclera contain the class I SLRPs, decorin and biglycan (Zhang et al., 2009). However, class II SLRPs demonstrate more variability in their distribution, lumican is expressed in both the corneal and scleral stroma while keratocan is present only in the corneal stroma. Fibromodulin is present in sclera, but is barely detectable/absent in the corneal stroma of adult mice (Chakravarti, 2002; Schonherr et al., 2004). Previous studies reported that fibromodulin-deficient mice had normal ocular axial length, while in compound lumican/fibromodulin-deficient mice axial length was increased. The phenotype in these double deficient mice is more severe than the phenotypes of the single gene-deficient mice (Chakravarti et al., 2003), suggesting a synergistic effect.

In the current work, we address the role (s) of fibromodulin in the regulation of region-specific fibrillogenesis required for the integration of the corneal and scleral matrices at the limbus and sulcus development required for normal vision. We hypothesize that fibromodulin modulates fibrillogenesis in a temporally and spatially restricted manner during postnatal development when the eye increases its axial length dramatically (Tkatchenko et al., 2009).

Results

Fibromodulin is expressed in the peripheral cornea during postnatal development

The presence of fibromodulin in the mature corneal stroma is controversial. To address this, fibromodulin expression was analyzed during corneal development and maturation using qPCR of epithelial stripped corneas. Fibromodulin mRNA was expressed at P4 and peaked at P14, at a level 4–5 times greater. This was followed by a precipitous decrease at P30 with

virtually no expression at P90 (Fig. 1A). Fibromodulin protein core exhibited a comparable expression pattern with peak levels at P14, a marked decrease at P30, and barely detectable levels at P90 as analyzed using semi-quantitative immuno-blots (Fig. 1B). These data indicate that fibromodulin is a stromal component during early corneal development, but not in the mature corneal stroma.

The spatial expression of fibromodulin was analyzed during corneal development and maturation using immunofluorescence microscopy. Fibromodulin was immuno-localized to the sclera, limbus and peripheral cornea at P4. Fibromodulin reactivity spread from the limbus to the central cornea at P14. However, by P30 reactivity had withdrawn to the peripheral corneal stroma and was mostly restricted to sclera after P60 (Fig. 2). Both the qPCR and semi-quantitative immune-blots were consistent with these changing expression patterns during development and maturation. These results suggested that fibromodulin may be involved in regulating fibrillogenesis in peripheral cornea during post-natal corneal development.

Differential expression patterns of lumican and fibromodulin in the limbus

Lumican and fibromodulin are closely related and interact physically with the same binding sites and may have coordinated expression patterns. To investigate the interactive function for these two SLRPs, the expression patterns of lumican and fibromodulin in cornea, sclera and limbus were analyzed using immunofluorescence microscopy. At P14, fibromodulin reactivity was strong in sclera; decreased in the peripheral cornea and limbus; and was weakly detected in cornea (Fig. 3A). Lumican showed a reciprocal spatial pattern. The unique overlapping pattern of lumican and fibromodulin expression in the limbus suggests that cooperation between these two SLRPs may contribute to tissue-specific functions in this region.

Lumican reactivity was increased in the limbus of fibromodulin-deficient mice

The SLRPs are closely related and compensatory effects need to be considered. For instance, biglycan can compensate for the loss of decorin in cornea (Zhang et al., 2009), and loss of fibromodulin leads to increased lumican in sclera and tendon (Svensson et al., 1999; Ezura et al., 2000; Chakravarti et al., 2003). To determine whether there were similar compensatory spatial increases in other SLRPs in fibromodulin-deficient mice immuno-histochemical analyses were performed using both wild type and fibromodulin-deficient mice. Lumican reactivity was increased in the peripheral cornea and limbus versus wild type. In contrast, no obvious changes were observed in reactivity of the closely related class II SLRP, keratocan (Fig. 3A, B). In fibromodulin null mice, there were no changes in reactivity or expression pattern for decorin and biglycan, class I SLRPs (Fig. 3C).

Fibromodulin regulates fibril growth in the limbus of the cornea during post-natal development

This study demonstrated that fibromodulin exhibited peak expression around P14 in the limbus/peripheral cornea. We didn't see obvious fibril structure changes in the central cornea in fibromodulin null mice compared to wild type mice. Therefore, the study was focused on the limbus, which is a transition region from corneal stroma to sclera architecture and this region is important in development of the sulcus and corneal curvature, both important in defining the optical axis and properties of the eye. The following regions were analyzed: the limbus, or junction between cornea and sclera. The corneal boundary of this region was defined as the site where the Descemet's membrane disappears. The peripheral zone of the posterior cornea stroma was analyzed ~30 μm from where the Descemet's membrane ends towards the central cornea (Fig. 4). Across the limbus, fibril structure and diameter gradually transition from the architecture characteristic of the sclera to that

characteristic of the corneal stroma. This pattern was similar between wild type mice and fibromodulin null mice. Our ultrastructural analyses demonstrated comparable circular fibril profiles and fibril diameter distributions in wild type and fibromodulin-deficient mice (Fig. 5). However, in fibromodulin-deficient mice during post-natal development, P4–P90, there is a shift to larger fibril diameters at P4–P14 relative to the wild type controls. In addition, the fibril diameter distribution developed a right shoulder indicating a population of larger diameter fibrils as well as a left shoulder indicating a population of smaller diameter fibrils at P30 in fibromodulin-deficient mice. Although a difference also was present at P90, the control and fibromodulin-deficient fibril distributions were more comparable at P90 than at P30. The changing fibrillar phenotypes in fibromodulin-deficient mice correlated with the changing expression levels of fibromodulin in the peripheral cornea during development. The results indicate that fibromodulin might play important roles during peripheral corneal development at P4–P30.

Interaction of lumican and fibromodulin during peripheral cornea development

The current work demonstrated that lumican reactivity was increased in the absence of fibromodulin in peripheral cornea and limbus. To investigate if lumican was involved in a cooperative interaction with fibromodulin in regulating fibrillogenesis, fibril structure and organization in the mid limbus (Fig. 6) were compared by transmission electron microscopy in P30 wild type mice, fibromodulin-deficient, lumican-deficient, and compound fibromodulin/lumican-deficient mice. Compared to fibromodulin-deficient mice, the fibril distribution in the mid limbus in compound fibromodulin, lumican-deficient mice showed a similar heterogeneous pattern, however, the whole distribution shifted to larger diameter fibril. The results indicated that both lumican and fibromodulin can prevent formation of larger diameter fibrils. The increased lumican reactivity may be associated with the increased incidence of smaller fibrils in the limbus in fibromodulin-deficient mice, and also may be responsible for the more comparable fibril distribution with wild type in fibromodulin-deficient mice at P14 than at P4 (Fig. 5).

In the posterior peripheral cornea, fibril profiles and diameter distributions were comparable in wild type mice and lumican-deficient mice. In contrast, the fibril diameter distribution in fibromodulin-deficient mice exhibited a right shoulder with larger diameter fibrils that was marginally significant relative to the wild type controls. The compound fibromodulin/lumican-deficient mice demonstrated a heterogeneous diameter distribution with significantly larger diameter fibrils. The large fibrils had altered fibril structures, with irregular/cauliflower profiles. These results indicate fibromodulin and lumican cooperate with each other in the regulation of lateral fibril growth in the peripheral cornea (Fig. 7).

Fibromodulin has similar core protein size in cornea, limbus and tendon

Fibromodulin was originally identified as a 59kDa protein bearing keratan sulfate glycosaminoglycan chains (Oldberg et al., 1989). However, different fibromodulin molecular weights have been reported in different tissues (Goldberg et al., 2009), 40kDa in dental tissue, 52 kDa in alveolar bone, and 59 kDa in tendon. Interestingly, fibromodulin null mice showed thicker fibrils in dental tissue, while thinner fibrils were found in tendon. Whether the different sizes of core proteins contribute to the different phenotype is unknown. To address this, mouse eyes were dissected into three parts: cornea; cornea/sclera junction including the limbus; and sclera. SLRPs were extracted and analyzed from these regions with and without deglycosylation with endo-β-galactosidase. The core proteins from all 3 ocular regions co-migrated in a position comparable to fibromodulin core protein from tendon after deglycosylation (Fig. 8). This data suggest that different phenotypes in sclera (Chakravarti et al., 2003) and peripheral cornea are not due to different core protein sizes. Fibromodulin from the corneal stroma also demonstrated a consistently broader band than in

the tendon or sclera indicating more size heterogeneity in the corneal fibromodulin. Similarly, lumican is glycosylated with keratan sulfate chains in the corneal stroma and is a glycoprotein in other tissues (Funderburgh et al., 1991; Cornuet et al., 1994). GAGs interactions can function to regulate interfibrillar spacing and organization through its hydration ability (Hayashida et al., 2006), but the function of core protein regulation of fibrils assembly does not require GAG chains (Zhang et al., 2009).

Our data are consistent with region-specific regulation of fibrillogenesis resulting from differential lumican and fibromodulin expression. This coordinate regulation is important in fine tuning the integration of the cornea and sclera which controls changes in eye shape and development of the optical axis critical for normal vision.

Discussion

This work defines an important regulatory role for fibromodulin in region-specific regulation of fibrillogenesis during the post-natal development of the limbus. This is a central site for integration of the cornea and sclera stromas; development of the sulcus and corneal curvature; as well as the optical properties of the anterior eye. Fibromodulin has important functions in regulating fibrillogenesis in different tissues such as tendon (Svensson et al., 1999; Ezura et al., 2000) and sclera (Chakravarti et al., 2003). Our data demonstrate unequivocally that fibromodulin is expressed in the cornea during postnatal development, but it is virtually absent in the adult cornea. Immuno-localization revealed a differential spatial and temporal expression pattern of fibromodulin during peripheral cornea development. Our analyses demonstrate that fibromodulin regulates fibrillogenesis in the peripheral cornea, where the sclera and corneal stromas are integrated during development, in a region specific manner.

The limbus is a transition zone between the strikingly different architectures of the corneal and scleral stromas. These two different connective tissues have different structural properties, e.g., rigidity and resilience. The distinct fibril structures in cornea and sclera also suggest changes in tensile strength across the limbus and peripheral cornea during development. Postnatal eye development is a tightly regulated process during emmetropization. Using high resolution small animal MRI, a recent study showed that murine eyes grow fastest prior to emmetropization, afterward, the eye expands its size slowly (Tkatchenko et al., 2009; Zieske, 2004). The unique temporal pattern of fibromodulin expression in the peripheral cornea is synchronized with this process during development. Accordingly, disruption of fibromodulin caused fibril disorganization; the most severe phenotype was around P30 during development. These data suggest that fibromodulin expression may be triggered by a change in mechanical stress in this transitional area during peripheral corneal development.

A change in the refractive power of the cornea has been observed to change dramatically at two stages, i.e., early development and aging. During infancy, the eye's refractive status transitions from hyperopia to emmetropization, the axial length increases while the corneal refractive power decreases. During later years of life, the axial length decreases, while cornea power increases. Although the axial length plays a major role in causing myopia, a number of studies have suggested that steepening of the cornea also is important for the development of myopia. The cornea is not mechanically inert; incisional refractive surgery can cause corneal curvature instability. Integrity of peripheral cornea refractive power has been shown to be important for normal vision (Grosvenor and Goss, 1998; Tabernero et al., 2009). The peripheral cornea, especially the limbus with predominantly circumferential arranged fibrils has been shown to be important in the stabilization of the corneal curvature.

In the cornea and sclera, SLRPs are differentially expressed. Decorin and biglycan are present in both, while keratocan is restricted to the cornea. Although lumican and fibromodulin were found in both the cornea and sclera stroma, lumican was predominantly in cornea, while fibromodulin was more prominent in the sclera. In the peripheral cornea, fibromodulin increased, while lumican decreased. In this overlap region, both fibromodulin and lumican single null mice had phenotypes comparable with wild type mice. The compound fibromodulin/lumican null mice demonstrated a severe fibril phenotype, which suggested a cooperative interaction between fibromodulin and lumican in regulation of fibril lateral assembly in this region. At the limbus, fibromudulin becomes dominant relative to weakly expressed lumican. Fibromodulin null mice showed both larger diameter and smaller diameter fibrils. Similar to our previous report in the sclera (Chakravarti et al., 2003), there was a subpopulation of smaller diameter fibrils at limbus in fibromodulin null mice. The smaller diameter fibrils were decreased in compound fibromodulin/ lumican null mice which suggested that the presence of lumican in the absence of fibromodulin contributes to maintenance of small diameter fibrils as in the corneal stroma in the fibromodulin-null mice. Lumican null mice are comparable with wild type mice at the limbus where lumican expression is weak compared with the corneal stroma. These results suggest that differential spatial expression of fibromodulin and lumican regulate fibrillogenesis in the transitional limbus between cornea and sclera. The results were consistent with our previous report that differential temporal expression of fibromodulin and lumican regulates fibrillogenesis in developing tendon (Ezura et al., 2000).

Fibromodulin and lumican share near 50% homology in sequence, binding to the same site on type I collagen fibrils and can inhibit each other in fibrillogenesis assay in vitro. In the peripheral cornea and limbus, fibromodulin null mice had larger diameter fibrils. In early tendon development a similar increase in diameter was observed (Ezura et al., 2000). However, later in tendon development, where fibromodulin expression is dominant and lumican is virtually absent, both fibromodulin null mice and compound fibromodulin/ lumican null mice had an increased proportion of smaller diameter fibrils. It was proposed that fibromodulin like lumican influences initial assembly of protofibrils similar to lumican, but also facilitates fibril maturation (Ezura et al., 2000). A recent report demonstrated that fibromodulin has two collagen binding LRR domains; One for initial cross linking, which is homologous to the lumican collagen binding site, and the other facilitating further assembly/ lateral fibril growth (Kalamajski and Oldberg, 2009). The major phenotype in limbus of fibromodulin null and compound fibromodulin /lumican null mice was a subpopulation of larger diameter fibrils. This was different from later stages in tendon development, although the fibromodulin/lumican ratio pattern was similar between these two tissues. The different phenotypes suggested that besides fibromodulin/lumican ratio, tissue specific factors such as other SLRPs, fibril associated collagens and adhesive glycoproteins also most likely contribute to the tissue-specific regulation (Zieske, 2004). Fibromodulin was recently reported to bind MMP-13 in vitro, which hypothetically may affect the collagen turnover (Tillgren et al., 2009). We noted that the phenotype is more severe in the peripheral region near cell processes (Fig. 6). This suggests that collagen turnover may be increased between P14–P30. Modulating matrix turnover also may be an important factor in regulating fibrillogenesis and matrix organization in these tissues (Oldberg et al., 2007).

Recent studies in human high myopia showed that Gly147Asp and Arg324Thr variations in fibromodulin were found in the highly conserved leucine-rich repeat (LRR) domains, which were thought as the genetic risk factors underlying the pathogenesis of high myopia (Majava et al., 2007). However, the ocular axial length was not changed in fibromodulin null mice (Chakravarti et al., 2003). Our data suggest that fibromodulin may be associated with myopia under pathological conditions; affecting the corneal and scleral curvature by regulating fibrillogenesis in the limbus region.

In conclusion, our study revealed a specific differential spatial and temporal expression of fibromodulin during peripheral cornea development. The temporal expression pattern was synchronized with emmetropization, the process in development whereby the eye increases its axial length and increases globe size dramatically. Our analysis demonstrated that fibromodulin regulates fibrillogenesis in a region specific manner in the peripheral cornea. This is the region where the corneal and sclera stromas are functionally integrated. Region-specific regulation of collagen fibrillogenesis during anterior eye development is required for the development of normal cornea curvature and normal vision.

Experimental Procedures

Animals

Gene targeted mice deficient in fibromodulin (Svensson et al., 1999; Ezura et al., 2000) or lumican (Chakravarti et al., 1998), as well as compound fibromodulin/lumican-null mice (Chakravarti et al., 2003) in a CD-1 background and wild type controls were utilized. Anterior eyes from mice at postnatal day 4 (P4), P14, P30 and P90 were used. Only males were analyzed except for P4 and P14 mice where sex was not determined. All animal studies were performed in compliance with IACUC approved animal protocols.

Analyses of mRNA expression

Expression of mRNA was measured essentially as previously described (Chakravarti et al., 2006). Briefly, corneas were dissected and the epithelia removed using dispase II (Roche). Total RNA was isolated from pooled corneas of wild type mice using Ribopure TM kits (Ambion). Independent cDNA preparations at each developing age were obtained by reverse transcription of series dilution of RNA (50ng, 10ng, 2ng, 0.4ng, 0.08ng, 0.016ng) with random primers (High-Capacity cDNA Archive Kit, Applied Biosystems, Foster City, CA). Real-time RT-PCR was performed using the LightCycler System (Invitrogen) with the SYBR Green PCR Master Mix (Applied Biosystems). Primer sequences for fibromodulin are: Forward primer: 5'-GAA GGG TTG TTA CGC AAA TGG -3'; Reverse primer: 5'-AGA TCA CCC CCT AGT CTG GGT TA- 3'. Actin was used as an endogenous control to standardize the amount of sample RNA. PCR amplification was done with cDNA derived RNA input for each sample used as template with primers concentrations of 50nm. The PCR cycle parameters were: 95°C 20 sec × 1 cycle, (95°C 3 sec, 60°C 30 sec) × 40 cycles.

Antibodies

Rabbit anti-decorin (LF113, provided by Dr. L. Fisher, NIH-NICDR) was used at 1:250, both anti-biglycan (LF159, provided by Dr. L. Fisher, NIH-NICDR) and anti-keratocan (provided by Dr. J. Hassell, USF Tampa, USA) were used at 1:200. Rabbit anti-lumican (provided by Dr. Ake Oldberg, Lund University, Sweden) was used at 1:1000. Rabbit anti-mouse fibromodulin (1:200, provided by provided by Dr. L. Fisher, NIH-NICDR) were used.

Immuno-localization analysis

Whole eyes were embedded in OCT medium, frozen on dry ice and stored at −80°C. Frozen sections (4μm) were cut using a HM 505E cryostat. Indirect immunofluoresence localization was performed as previously described (Chen et al., 2008). For fibromodulin immunofluorecence localization, sections were pretreated with Chondroitinase ABC (Seikagaku Biobusiness Corporation) at 0.2u/ml at 37 °C for 1 hour, followed by applying the primary antibody. The secondary antibody was Alexa Fluor 568 or 488-conjugated goat anti rabbit IgG (Molecular Probes, Eugene, OR) used at 1:100. Vectashield mounting solution with DAPI (Vector Laboratories, Inc., Burlingame, CA) was used as a nuclear

marker. Negative control samples were incubated identically, except the primary antibody was excluded. Images were captured using a Leica CTR 5500 microscope and Leica DFC 340 FX camera. Identical conditions and set integration times were used to facilitate comparisons between samples.

Immuno-blots

Specific regions or tissues were dissected from animals at P4, P14, P30, P90, and pooled followed by homogenizing in 20 fold excess (weight/volume) of extraction buffer (4 M guanidine-HCl, 50 mM sodium acetate, pH 5.8) with proteinase inhibitor (Thermo Scientific). Small leucine rich proteoglycans were extracted at 4°C for 48 hours with shaking. The extraction was clarified by centrifugation and then dialyzed against 150 mM Tris-HCl, 150mM NaCl pH 7.3. Samples were digested with chondroitinase ABC or endo-beta-galacosidase (Seikagaku Biobusiness Corporation) for 24 hours at 37°C (Zhang et al., 2009). Total protein concentration was determined using BCA protein assay kit (Pierce). Proteins from each preparation were and run through 4–12% bis-tris gel (Invitrogen) and transferred to membrane for immunoblotting. Goat anti-rabbit IgG-perixodase (Amersham) was used as secondary antibody at 1:3000 with an ECL (Pierce) detection system. Actin reactivity in each sample was detected using an anti-actin antibody (Chemicon).

Transmission electron microscopy

Cornea samples from wild type, *Fmod*$^{-/-}$, *Lum*$^{-/-}$, and *Fmod*$^{-/-}$ /*Lum*$^{-/-}$ mice at P14, P30 and P90 were analyzed by transmission electron microscopy as previously described (Zhang et al., 2009). Briefly, the cornea along with the anterior sclera were dissected and fixed in 4% paraformaldehyde, 2.5% glutaraldehyde, 0.1 M sodium cacodylate pH 7.4, with 8.0 mM $CaCl_2$, post-fixed with 1% osmium tetroxide. They were dehydrated in an ethanol series, followed by propylene oxide. The tissue samples were infiltrated and embedded in a mixture of EMbed 812, nadic methyl anhydride, dodecenyl succinic anhydride and DMP-30 (Electron Microscopy Sciences, Hatfield, PA.). Thin sections (80nm) were cut using a Leica ultramicrotome and post-stained with 2% aqueous uranyl acetate and 1% phosphotungstic acid, pH 3.2. The peripheral cornea and limbus were examined at 80 kV using a JEOL 1400 transmission electron microscope equipped with a Gatan Ultrascan US1000 2 K digital camera.

Fibril Diameter Distribution

Five corneas from three to five different animals at P4, P14, P30, P90 were analyzed for each genotype: *Fmod*−/−, *Lum*−/−, *Fmod* −/− *Lum* −/− and wild type control. Digital images (9/group) were taken from non-overlapping regions. The following regions were analyzed: the limbus, or junction between cornea and sclera. The corneal boundary of this region was defined as the site where the Descemet's membrane ends. The peripheral zone of the posterior cornea stroma was analyzed ~30 μm from where the Descemet's membrane disappears towards central cornea. Fibril diameters were measured with a RM Biometrics-Bioquant Image Analysis System (Nashville, TN) using randomly chosen, masked digital images analyzed at a final magnification of 48,000X. For each of the group, sample mean, sample median-to-first quartile distance (M-Q1), and sample third quartile distance to median (Q3-M), were analyzed. The median indicates the location of the center of the distribution, while median-to-quartile distances reflect primarily the spread of the data. Distributions of the sample to sample means and both median-to-quartile distances for each deficient group were compared with the wild-type group using the T- test.

Acknowledgments

Grant Sponsor: NIH/NEI; EY05129 and EY11654.

We gratefully acknowledge Sheila Adams, Nikola Valkov and Mei Sun for the expert advice and technical assistance. We thank Simone Smith, Michael Mienaltowski and John Fitch for their input on the manuscript.

References

Bredrup C, Knappskog PM, Majewski J, Rodahl E, Boman H. Congenital stromal dystrophy of the cornea caused by a mutation in the decorin gene. Invest Ophthalmol Vis Sci. 2005; 46:420–426. [PubMed: 15671264]

Carlson EC, Liu CY, Chikama T, Hayashi Y, Kao CW, Birk DE, Funderburgh JL, Jester JV, Kao WW. Keratocan, a cornea-specific keratan sulfate proteoglycan, is regulated by lumican. J Biol Chem. 2005; 280:25541–25547. [PubMed: 15849191]

Chakravarti S. Functions of lumican and fibromodulin: lessons from knockout mice. Glycoconj J. 2002; 19:287–293. [PubMed: 12975607]

Chakravarti S, Magnuson T, Lass JH, Jepsen KJ, LaMantia C, Carroll H. Lumican regulates collagen fibril assembly: skin fragility and corneal opacity in the absence of lumican. J Cell Biol. 1998; 141:1277–1286. [PubMed: 9606218]

Chakravarti S, Paul J, Roberts L, Chervoneva I, Oldberg A, Birk DE. Ocular and scleral alterations in gene-targeted lumican-fibromodulin double-null mice. Invest Ophthalmol Vis Sci. 2003; 44:2422–2432. [PubMed: 12766039]

Chakravarti S, Zhang G, Chervoneva I, Roberts L, Birk DE. Collagen fibril assembly during postnatal development and dysfunctional regulation in the lumican-deficient murine cornea. Dev Dyn. 2006; 235:2493–2506. [PubMed: 16786597]

Chen S, Wassenhove-McCarthy DJ, Yamaguchi Y, Holzman LB, van Kuppevelt TH, Jenniskens GJ, Wijnhoven TJ, Woods AC, McCarthy KJ. Loss of heparan sulfate glycosaminoglycan assembly in podocytes does not lead to proteinuria. Kidney Int. 2008; 74:289–299. [PubMed: 18480751]

Cornuet PK, Blochberger TC, Hassell JR. Molecular polymorphism of lumican during corneal development. Invest Ophthalmol Vis Sci. 1994; 35:870–877. [PubMed: 8125750]

Danielson KG, Baribault H, Holmes DF, Graham H, Kadler KE, Iozzo RV. Targeted disruption of decorin leads to abnormal collagen fibril morphology and skin fragility. J Cell Biol. 1997; 136:729–743. [PubMed: 9024701]

Derdoy J. Degenerative myopia: Scleral collagenopathy? Arch Oftalmol B Aires. 1968; 43:118–122. [PubMed: 5719323]

Ezura Y, Chakravarti S, Oldberg A, Chervoneva I, Birk DE. Differential expression of lumican and fibromodulin regulate collagen fibrillogenesis in developing mouse tendons. J Cell Biol. 2000; 151:779–788. [PubMed: 11076963]

Funderburgh JL, Funderburgh ML, Mann MM, Conrad GW. Arterial lumican. Properties of a corneal-type keratan sulfate proteoglycan from bovine aorta. J Biol Chem. 1991; 266:24773–24777. [PubMed: 1761572]

Goldberg M, Ono M, Septier D, Bonnefoix M, Kilts TM, Bi Y, Embree M, Ameye L, Young MF. Fibromodulin-deficient mice reveal dual functions for fibromodulin in regulating dental tissue and alveolar bone formation. Cells Tissues Organs. 2009; 189:198–202. [PubMed: 18698127]

Goldberg M, Septier D, Oldberg A, Young MF, Ameye LG. Fibromodulin-deficient mice display impaired collagen fibrillogenesis in predentin as well as altered dentin mineralization and enamel formation. J Histochem Cytochem. 2006; 54:525–537. [PubMed: 16344330]

Grosvenor T, Goss DA. Role of the cornea in emmetropia and myopia. Optom Vis Sci. 1998; 75:132–145. [PubMed: 9503439]

Hayashida Y, Akama TO, Beecher N, Lewis P, Young RD, Meek KM, Kerr B, Hughes CE, Caterson B, Tanigami A, Nakayama J, Fukada MN, Tano Y, Nishida K, Quantock AJ. Matrix morphogenesis in cornea is mediated by the modification of keratan sulfate by GlcNAc 6-O-sulfotransferase. Proc Natl Acad Sci U S A. 2006; 103:13333–13338. [PubMed: 16938851]

Kalamajski S, Oldberg A. Homologous sequence in lumican and fibromodulin leucine-rich repeat 5–7 competes for collagen binding. J Biol Chem. 2009; 284:534–539. [PubMed: 19008226]

Majava M, Bishop PN, Hagg P, Scott PG, Rice A, Inglehearn C, Hammond CJ, Spector TD, Ala-Kokko L, Mannikko M. Novel mutations in the small leucine-rich repeat protein/proteoglycan (SLRP) genes in high myopia. Hum Mutat. 2007; 28:336–344. [PubMed: 17117407]

Matheson S, Larjava H, Hakkinen L. Distinctive localization and function for lumican, fibromodulin and decorin to regulate collagen fibril organization in periodontal tissues. J Periodontal Res. 2005; 40:312–324. [PubMed: 15966909]

Oldberg A, Antonsson P, Lindblom K, Heinegard D. A collagen-binding 59-kd protein (fibromodulin) is structurally related to the small interstitial proteoglycans PG-S1 and PG-S2 (decorin). EMBO J. 1989; 8:2601–2604. [PubMed: 2531085]

Oldberg A, Kalamajski S, Salnikov AV, Stuhr L, Morgelin M, Reed RK, Heldin NE, Rubin K. Collagen-binding proteoglycan fibromodulin can determine stroma matrix structure and fluid balance in experimental carcinoma. Proc Natl Acad Sci U S A. 2007; 104:13966–13971. [PubMed: 17715296]

Pellegata NS, Dieguez-Lucena JL, Joensuu T, Lau S, Montgomery KT, Krahe R, Kivela T, Kucherlapati R, Forsius H, de la Chapelle A. Mutations in KERA, encoding keratocan, cause cornea plana. Nat Genet. 2000; 25:91–95. [PubMed: 10802664]

Rada JA, Shelton S, Norton TT. The sclera and myopia. Exp Eye Res. 2006; 82:185–200. [PubMed: 16202407]

Rodahl E, Van Ginderdeuren R, Knappskog PM, Bredrup C, Boman H. A second decorin frame shift mutation in a family with congenital stromal corneal dystrophy. Am J Ophthalmol. 2006; 142:520–521. [PubMed: 16935612]

Schaefer L, Iozzo RV. Biological functions of the small leucine-rich proteoglycans: from genetics to signal transduction. J Biol Chem. 2008; 283:21305–21309. [PubMed: 18463092]

Svensson L, Aszodi A, Reinholt FP, Fassler R, Heinegard D, Oldberg A. Fibromodulin-null mice have abnormal collagen fibrils, tissue organization, and altered lumican deposition in tendon. J Biol Chem. 1999; 274:9636–9647. [PubMed: 10092650]

Svensson L, Narlid I, Oldberg A. Fibromodulin and lumican bind to the same region on collagen type I fibrils. FEBS Lett. 2000; 470:178–182. [PubMed: 10734230]

Tabernero J, Vazquez D, Seidemann A, Uttenweiler D, Schaeffel F. Effects of myopic spectacle correction and radial refractive gradient spectacles on peripheral refraction. Vision Res. 2009; 49:2176–2186. [PubMed: 19527743]

Tillgren V, Onnerfjord P, Heinegard D. The tyrosine sulfate rich domains of the LRR-proteins fibromodulin and osteoadherin bind motifs of basic clusters in a variety of heparin binding proteins including bioactive factors. J Biol Chem. 2009

Tkatchenko TV, Shen Y, Tkatchenko AV. Analysis of Postnatal Eye Development in the Mouse with High-Resolution Small Animal MRI. Invest Ophthalmol Vis Sci. 2009

Wang IJ, Chiang TH, Shih YF, Hsiao CK, Lu SC, Hou YC, Lin LL. The association of single nucleotide polymorphisms in the 5'-regulatory region of the lumican gene with susceptibility to high myopia in Taiwan. Mol Vis. 2006; 12:852–857. [PubMed: 16902402]

Zhang G, Chen S, Goldoni S, Calder BW, Simpson HC, Owens RT, McQuillan DJ, Young MF, Iozzo RV, Birk DE. Genetic evidence for the coordinated regulation of collagen fibrillogenesis in the cornea by decorin and biglycan. J Biol Chem. 2009; 284:8888–8897. [PubMed: 19136671]

Zieske JD. Corneal development associated with eyelid opening. Int J Dev Biol. 2004; 48:903–911. [PubMed: 15558481]

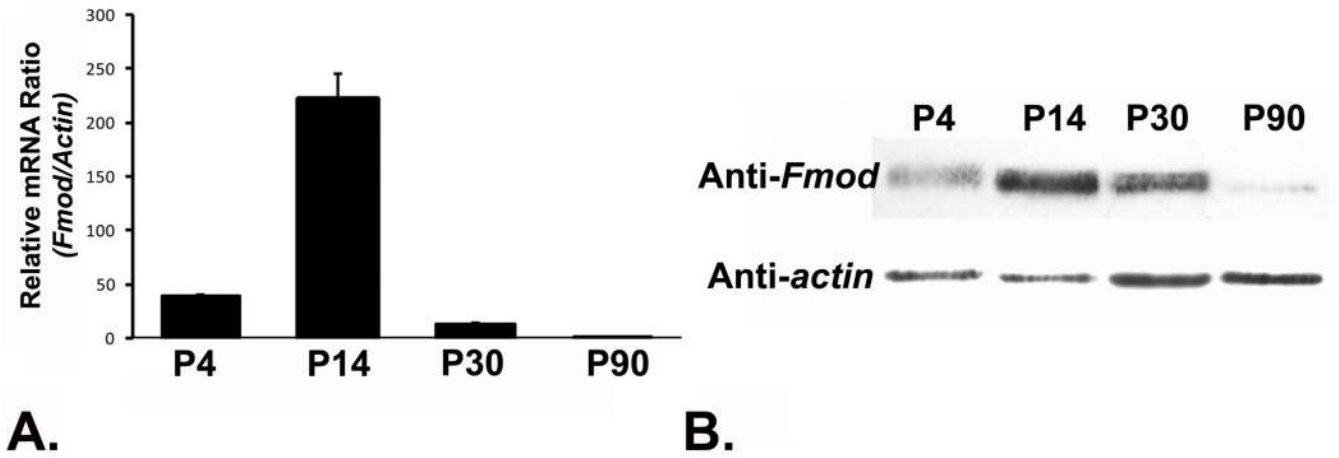

Figure 1. Fibromodulin is expressed in the stroma during postnatal corneal development

(A) Fibromodulin is expressed during post-natal corneal development, but not in the mature corneal stroma. Fibromodulin mRNA expression was highest at P14 and decreased markedly at P30 with virtually no expression at P90. The cornea was dissected from mice at different developmental stages indicated, followed by epithelial stripping and mRNA was extracted from pooled corneas. Relative fibromodulin expression is shown as the ratio of *Fmod*/actin mRNA detected by realtime PCR. **(B)** Fibromodulin core protein expression in the corneal stroma was comparable to the mRNA expression pattern analyzed using semi-quantitative immuno- blots. Highest fibromodulin expression was at P14, there was a decrease at P30 and at P90, fibromodulin was barely detected. Sample was extracted and followed by deglycosylation with endo-β-galactosidase, actin was included as a loading control.

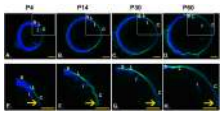

Figure 2. Differential spatial and temporal expression of fibromodulin during peripheral cornea development

A differential expression of fibromodulin in the limbus/peripheral cornea was observed by immuno-fluorescence analysis of different developmental stages (P4–P60). **(A)** Fibromodulin (green) reactivity was detected weakly around the limbus at P4. **(B)** Reactivity was significantly enhanced and extended into the central cornea at P14. **(C)** The reactivity for fibromodulin began to "retract" to the limbus at P30 and **(D)** decreased in the peripheral cornea at P60. **(E– H)** are higher magnifications of the areas indicated by the white box in **(A– D)**. Blue, DAPI for nuclear localization; green, anti-fibromodulin; S: Sclera; L: limbus; I: iris; C: cornea, yellow arrow indicates central cornea. Bars=500 μm. (Panel A, B, C, D are montages created from images with the same exposure).

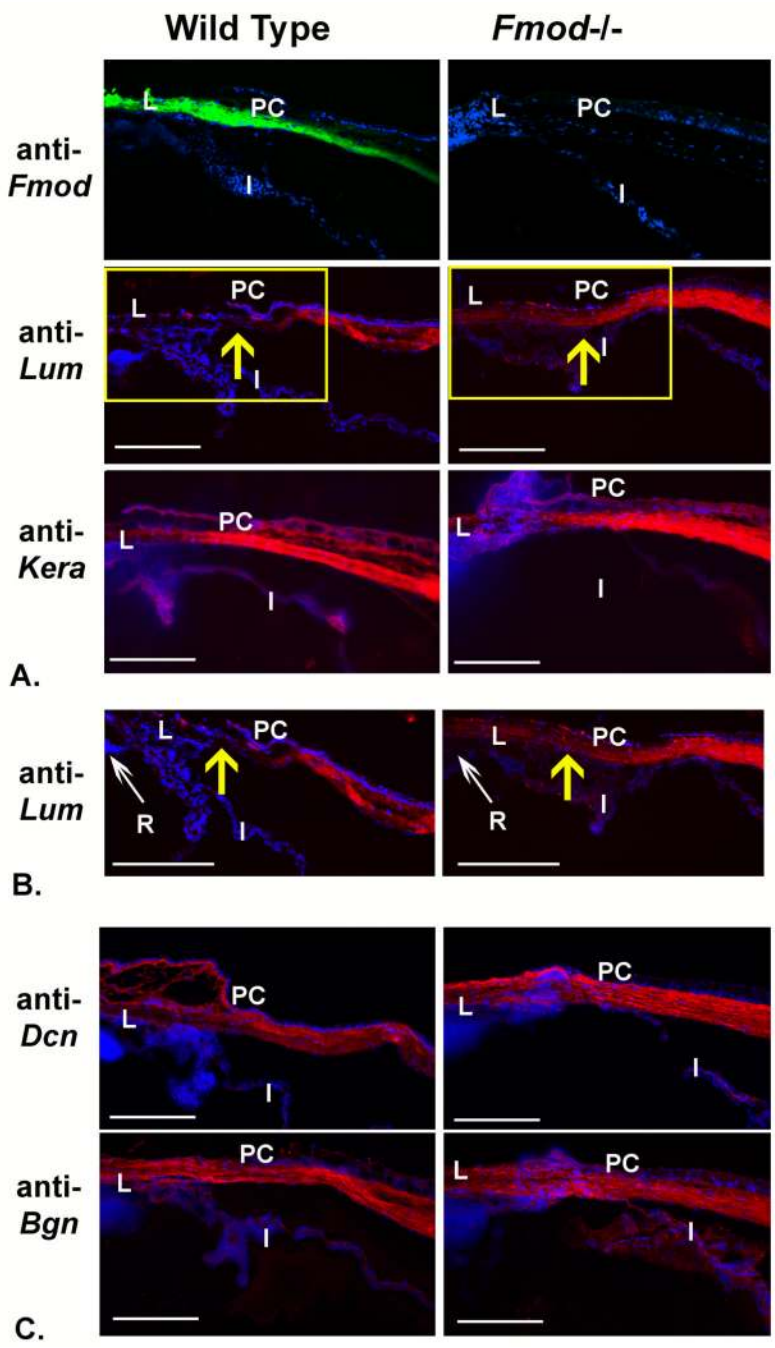

Figure 3. Increased lumican in limbus/peripheral cornea of fibromodulin-deficient mice

(A) Lumican and fibromodulin were differentially expressed in cornea, limbus/peripheral cornea as analyzed by immuno-fluorescence microscopy. Fibromodulin reactivity was prominent in sclera and limbus, but also extended into the peripheral cornea during development. Lumican and keratocan were restricted to the peripheral cornea around the limbus. In fibromodulin-deficient mice, Lumican reactivity was increased in the peripheral cornea (yellow rectangle and arrow, enlarged in **(B)**. **(C)** Decorin and biglycan were homogenously distributed across cornea and sclera stroma, no obvious changes were observed in either expression pattern or intensity from decorin, biglycan and keratocan. (L: limbus; I: iris; PC: peripheral cornea: R: retina. Bar=200μm)

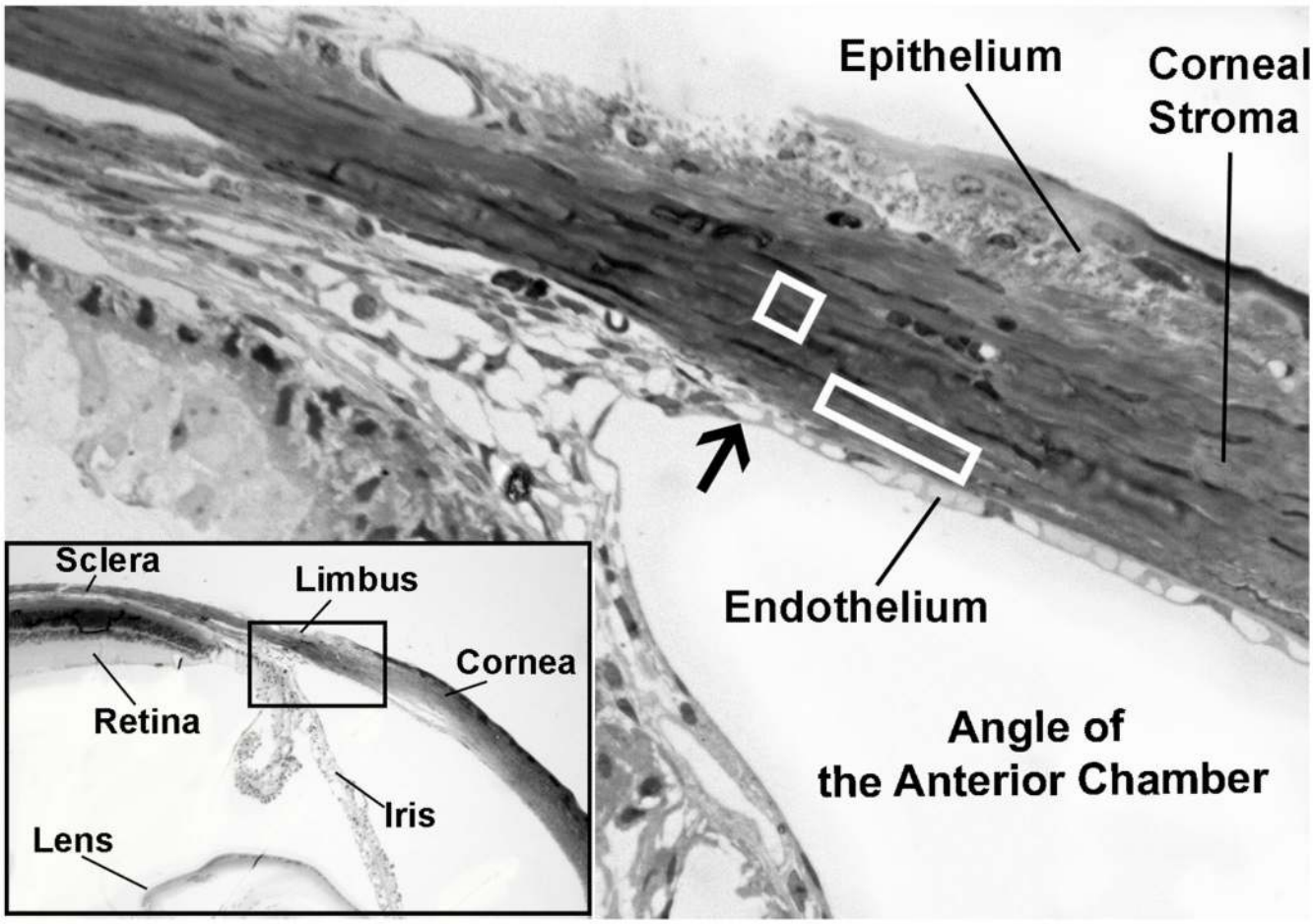

Figure 4. Light microscopy of the limbus of the anterior eye

The transparent cornea joins the opaque sclera at the limbus. The endothelium of the cornea is continuous with the epithelial lining of the angle of anterior chamber. The point where Decemet's layer disappears is defined as the lateral boundary of the endothelium and beginning of the limbus (indicated by black arrow). The following regions were analyzed: the limbus, or junction between cornea and sclera (white square, Fig. 5, 6). The peripheral zone of the posterior cornea stroma was analyzed ~30 μm from where the Descemet's layer ends towards the central cornea (white rectangle, Fig. 7).

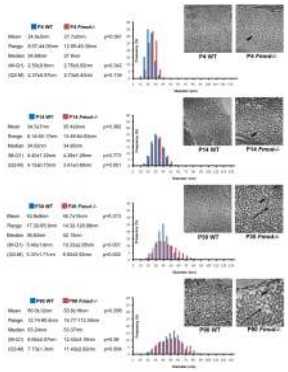

Figure 5. Fibromodulin regulates post-natal fibril growth in the limbus during development

Ultrastructural analyses demonstrated comparable circular fibril profiles in wild type and fibromodulin-deficient mice, with the fibril distribution shifted to larger diameters at both P4 and P14. Significantly, the fibril distribution demonstrated both right and left shoulders in fibromodulin−/− mice at P30, indicating an increased subpopulation of larger (thicker arrow) as well as smaller fibrils (thin arrow) at the limbus. Although the difference existed at P90, the control and fibromodulin−/− fibril distributions were closer at P90 than at P30. (M: median; Q1: 25 percentile; Q3: 75 percentile; Bar=200nm)

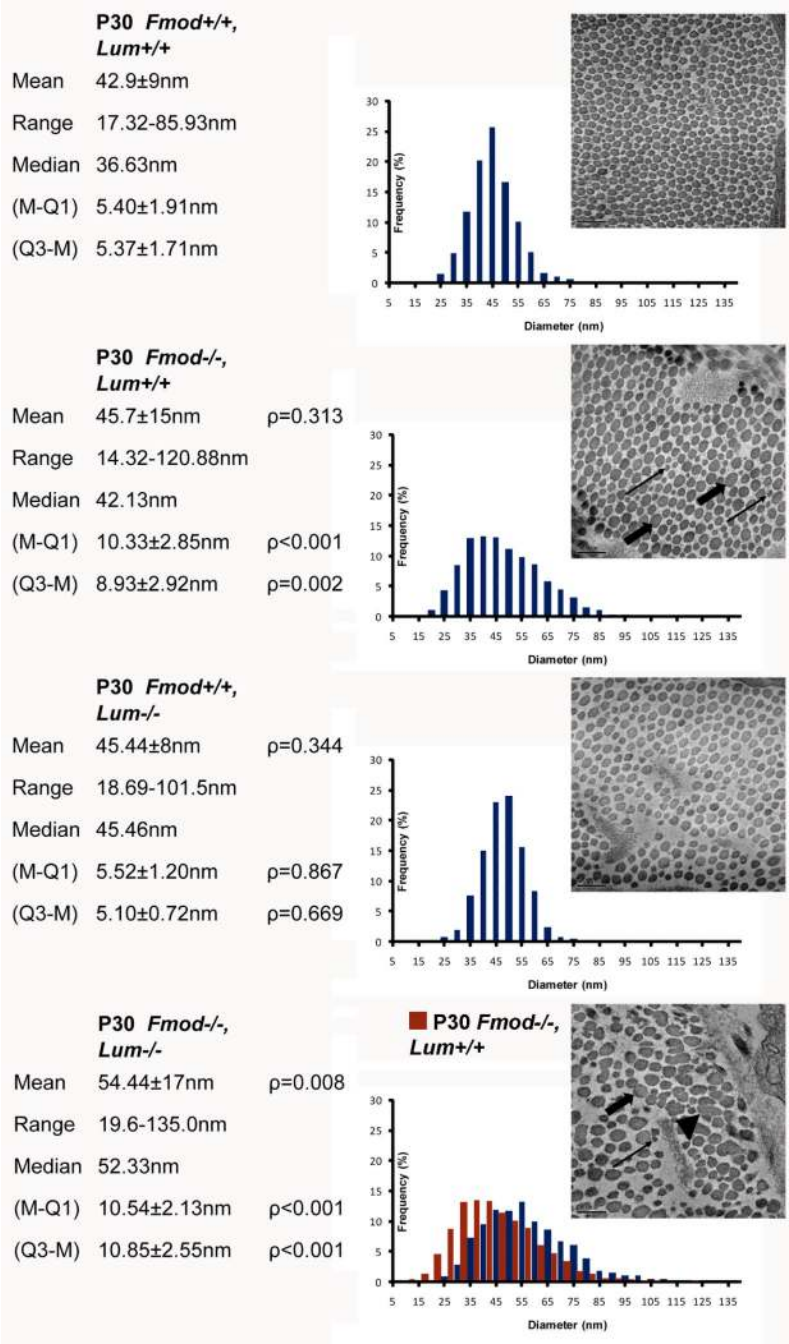

Figure 6. Increased lumican expression is associated with an increase in smaller diameter fibrils in the limbus of fibromodulin-deficient mice

Both fibromodulin−/− mice and compound fibromodulin/lumican null mice showed similar heterogeneous diammeter distributions, however, the distribution in compound null mice was shifted to the right compared to fibromodulin-deficient mice. While Lumican-deficient mice showed structures comparable to wild type mice as demonstrated by ultrastructure analyses performed at mid stroma in the limbus. (Thin arrow: smaller diameter fibril; thicker arrow: larger diameter fibril; triangle: deformed fibril with cauliflower contour; M: median; Q1: 25 percentile; Q3: 75 percentile; Bar= 200nm)

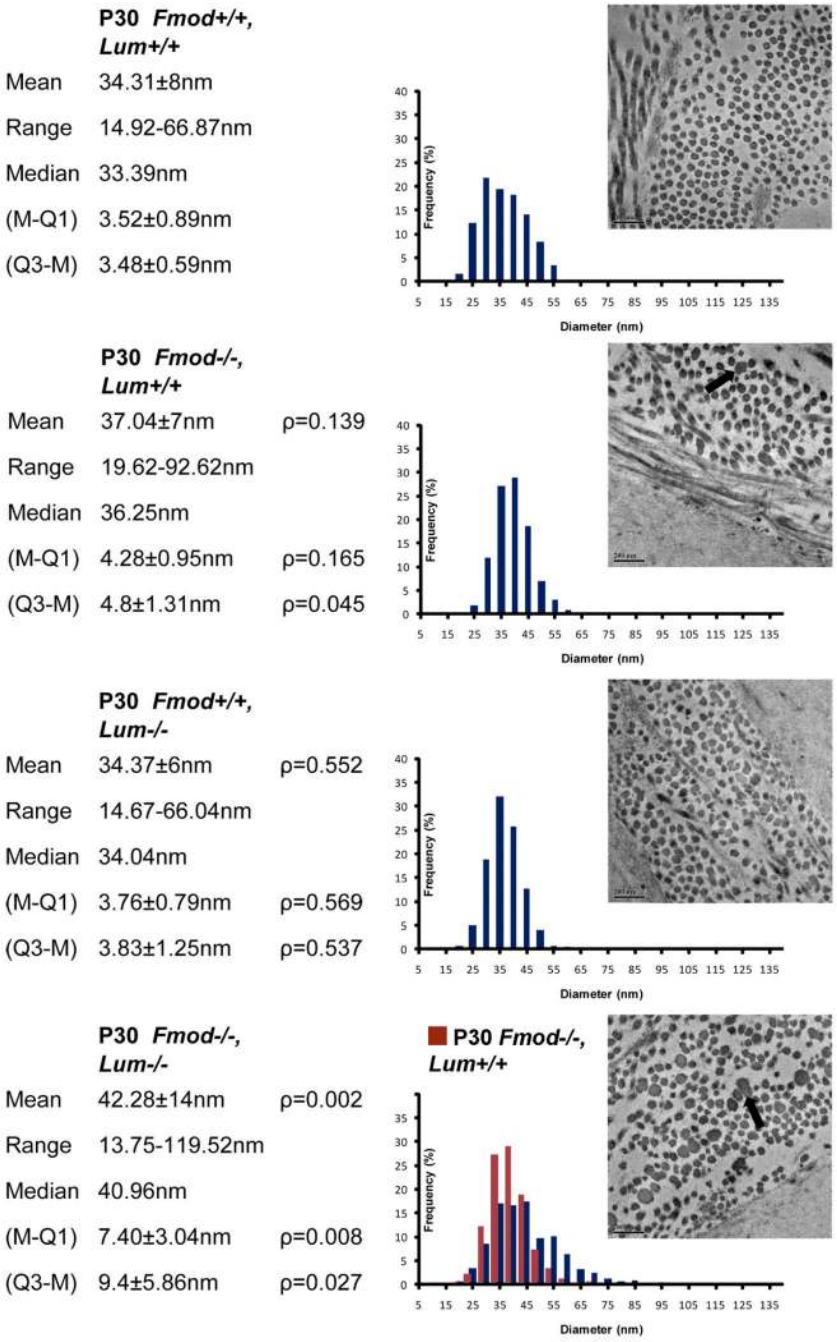

Figure 7. Cooperative interaction of fibromodulin and lumican in regulation of fibrillogenesis at the peripheral posterior corneal stroma adjacent to the limbus

Significantly larger diameter fibrils, with cauliflower like contours were present in compound fibromodulin/lumican null mice, while lumican-deficient mice showed comparable fibril structures to control. Fibromodulin null mice showed a marginal shift to the right compared to wild type mice as shown by ultrastructure analysis in marginal zone of peripheral posterior cornea near limbus. (Thick arrow: larger diameter fibril. M: median; Q1: 25 percentile; Q3: 75 percentile; Bar=200nm)

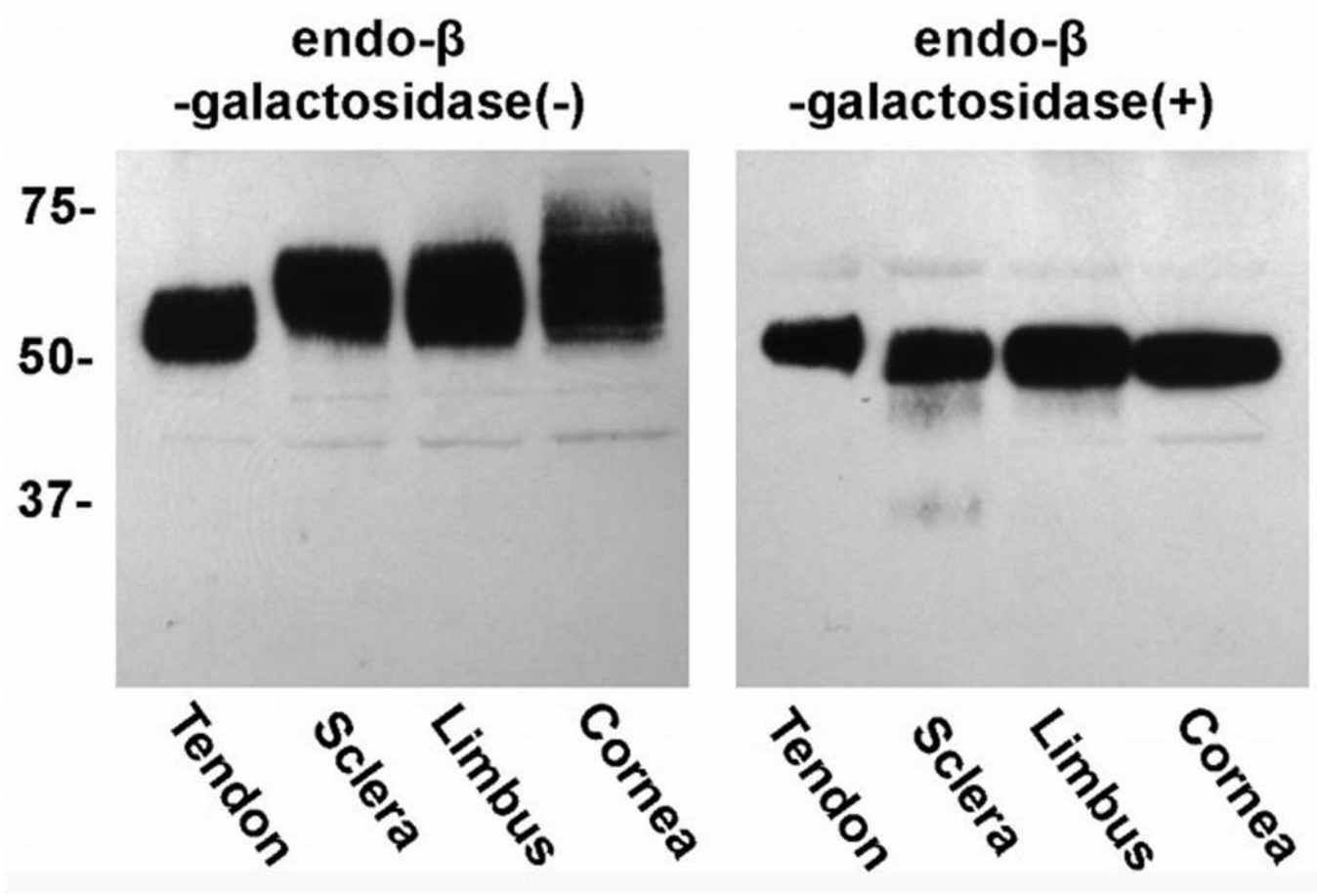

Figure 8. Fibromodulin has similar size of core protein in cornea, limbus and sclera

SLRPs were extracted from tendon, sclera, limbus and cornea separately and analyzed using immuno-blots with and without deglycosylation using endo-β-galactosidase. The core proteins from all 3 ocular regions co-migrated in a position comparable to fibromodulin core protein from tendon after deglycosylation. However, analysis of the non-deglycosylated fibromodulin demonstrated slower migrating bands relative to fibromodulin from tendon in all 3 ocular regions. In addition, fibromodulin from the corneal stroma demonstrated a consistently broader band than in the limbus or sclera indicating more size heterogeneity in the corneal fibromodulin. Equal protein (2μg) was loaded in each lane. (*Limbus: limbus rich region was contaminated with both cornea and sclera).